Numerical Simulation of DSC and TMDSC Curves as Well as Reversing and Nonreversing Curve Separation

Jinan Cao

Faculty of Engineering and Industrial Sciences, Swinburne University of Technology, Hawthorn, Victoria 3122, Australia

Received 17 July 2006; accepted 7 March 2007
DOI 10.1002/app.26787
Published online 13 August 2007 in Wiley InterScience (www.interscience.wiley.com).

ABSTRACT: The basic physical meaning of temperature modulation for DSC is an arguable research topic, and its interpretation affects the development of thermal analysis and polymer science. This article studies the basic physical meaning of TMDSC by numerical simulation. DSC and TMDSC output curves are computed for a sample with step changes in its specific heat and for a sample with crystallites melting over the temperature range. The TMDSC curves are further analyzed to obtain the reversing and nonreversing components. It is shown that separation of the reversing and nonreversing components from the underlying heat flow cannot be justified. Some common misconceptions regarding TMDSC are discussed as well. © 2007 Wiley Periodicals, Inc. J Appl Polym Sci 106: 3063–3069, 2007

Key words: TMDSC; reversing component; nonreversing component; phase lag

INTRODUCTION

DSC is the most comprehensive and popular instrumental technique used in thermal characterization of materials, in particular of polymers. In a conventional DSC, the heating block has a linear temperature scanning program where the heat flow difference between the sample and reference is measured and calculated as output. Reading invented temperature modulated DSC (TMDSC) in 1993, in which a sinusoidal temperature modulation is superimposed on the linear temperature program.[1,2] TMDSC has then become a popular topic of research.[3–11] Different names such as alternating DSC (ADSC), modulated DSC (MDSC), and modulated temperature DSC (MTDSC) were once used for TMDSC. Sawtooth temperature variation, often called dynamic DSC (DDSC), can also be employed as an alternative modulation.

It is true that a linear temperature scanning program is a special case of a modulated scanning program. This fact has invited one to readily believe that there are intrinsic merits of TMDSC over conventional DSC, because a TMDSC can obviously be used as a normal DSC when the amplitude of temperature modulation is set at zero. This is correct from the point of view of instrumentation technology and stimulated a rapid development for new instruments. However, one may not realize that it is only when the amplitude is set at zero (constant hearing rate) that the output is free from unwanted instrumental factors. TMDSC have been addressed in the past decade but fundamental questions remain unanswered: what are the additional physical quantities deriving from TMDSC? Do these additional physical quantities originate from test materials/samples, or originate from the specific way of TMDSC measurements? We now need a rational comprehensive understanding of TMDSC, one way or the other.

Complication of TMDSC comes from the entanglement of three principal factors. The first is the principle of measurement of TMDSC, the second is the complexity of test materials, usually polymers, and the third is the experimental limitations. The lack of understanding of the principle of TMDSC facilitates erroneous interpretations of the complexity of test materials on one hand; the complexity of test materials leaves room for false accounts for the principle of TMDSC on the other. This is further compounded with the experimental limitations that always contain errors but the principle of TMDSC measurement does not take the experimental errors into account.

Numerical experiments simulating complete DSC and TMDSC curves, and therefore are crucial because of its capability to disentangle above-mentioned three factors. By assuming a sample having certain relevant properties, one can conduct numerical simulations that determine output accurately and precisely, which in turn, reveals naked principles of TMDSC measurements.

Correspondence to: J. Cao (jcao@swin.edu.au).

Journal of Applied Polymer Science, Vol. 106, 3063–3069 (2007)

In two previous articles of the author, the full mathematical equations of DSC and TMDSC have been formulized and the numerical method established to obtain complete DSC and TMDSC curves for heat capacity measurement, crystallization, and melting processes.[12,13] This article will specifically address subsequent analysis/interpretation of the raw TMDSC output curves, in particular, how the reversing and nonreversing components are generated in TMDSC, which plays a crucial role in concluding what the reversing and nonreversing components stand for. Note that this simulation of reversing and nonreversing components differs fundamentally from the approach by Xu et al.[14] who input an artificial nonreversing heat flow in their simulation, therefore not able to elucidate the nature of the reversing and nonreversing components of TMDSC output.

THEORY/BACKGROUND

The governing equation of TMDSC

The governing equation for TMDSC reads

$$\frac{dT(t)}{dt} + \frac{\lambda}{C_p} T(t) = \frac{\lambda}{C_p} [T_{b_0} + qt + A_b \sin \omega t] \qquad (1)$$

where $T(t)$ denotes temperature at time t; T_{b_0} the initial temperature of the heating block; q, A_b, and ω represent the underlying heating rate, the amplitude, and angular frequency of modulation, respectively ($\omega = 2\pi/p$, where p is the modulation period), and C_p is the heat capacity. $T(t)$, and C_p can have a subscript s or r to denote sample or reference. The symbol λ describes the thermal transfer coefficient between the heating block and sample and reference, which is determined by the design and construction of a particular instrument, also affected by other factors such as the type of sample holder. λ is considered to be identical for sample and reference, and a constant during a run.[3,12,13]

The initial conditions of DSC and TMDSC experiments

The complete curves of a DSC and TMDSC experiment can be obtained by solving the governing equation incorporating relevant initial conditions. For simplicity, the initial temperatures for the sample, reference, and heating block are assumed identical being at room temperature, 20°C. For a generalized case that contains discontinuous changes either in the heat capacity of the sample or in the heating rate (e.g., saw-tooth modulation for DDSC) in an experiment, integration of the governing equation has to be carried out from range to range successively.[12]

Analytical solutions and numerical solutions

The governing equation is analytically solvable when there are only step changes in the specific heat of a sample and/or in the heating rate (saw-tooth modulation). The heat flow at the ith range is written as:[12,13]

$$H_f^i(t) = \lambda \left(C_r \exp\left(-\frac{\lambda t}{C_{\mathrm{pr}}} \right) - C_s^i \exp\left(-\frac{\lambda (t - t_i)}{C_{\mathrm{ps}}^i} \right) \right) + q\left(C_{\mathrm{ps}}^i - C_{\mathrm{pr}}\right) + H_f^{mi}(t) \qquad (2)$$

where $H_f^{\mathrm{mi}}(t)$ denotes the modulation component, which reads

$$H_f^{\mathrm{mi}}(t) = \left(\frac{A_b \left(C_{\mathrm{ps}}^i - C_{\mathrm{pr}}\right) \lambda^2 \omega}{\sqrt{(C_{\mathrm{ps}}^{i2}\omega^2 + \lambda^2)(C_{\mathrm{pr}}^2\omega^2 + \lambda^2)}} \right) \sin(\omega t - \delta) \qquad (3)$$

where δ is the phase shift defined as

$$\delta = \tan^{-1}\left(\frac{C_{\mathrm{ps}}^i C_{\mathrm{pr}} \omega^2 - \lambda^2}{\lambda \omega \left(C_{\mathrm{ps}}^i + C_{\mathrm{pr}}\right)} \right) \qquad (4)$$

C_s^i and C_r are constants; t_i the time at which the sample reaches the starting temperature of the ith range. For a saw-tooth modulation, eq. (2) holds without the term, $H_f^{mi}(t)$.[12]

In a previous publication, eq. (3) was not in this simplest form but a little bit more complicated [eq. (11) in Ref. 12]. This simplest form was presented at the Fifth Lhnwitz Seminar on Calorimetry in Germany in 1998.[15] The conclusion that the amplitude of heat flow is a nonlinear function of the thermal transfer coefficient, λ, the modulation period, p, the heat capacity of reference, C_{pr}, and the hear capacity of a sample, C_{ps}, is true. By finding this simpler form, Clarke et al.[16] argued that the amplitude of the heat flow is a function of the heat capacity of a sample, C_{ps}. Certainly nonlinear function is a function; therefore, the argument is really invalid.

Both the phase lag and the amplitude are a function of the thermal transfer coefficient, λ, adding one more parameter into the measurement. λ is an instrumental factor, being not what we wish to measure, but what we try to avoid. DSC does not work without λ. There is no exaggeration to say that the smartest innovation in the history of thermal analysis is the cancellation of λ and C_{pr} in DSC output signal that is achieved by ''differential,'' using an identical reference. TMDSC moves backward bringing the two instrumental factors back to the output of TMDSC.

TABLE I
Measurement Conditions and Thermal Properties of the Sample

Thermal transfer coefficient λ (J/K s)	Underlying heating rate q (°C/min)	Amplitude of modulation A_b (°C)	Modulation period p (s)	Heat capacity of reference C_{pr} (J/K)	Mass of sample (mg)	Specific heat of sample c_{ps} (J/gK) heat capacity of sample C_{ps} (J/K)		
						Range 0	Range I	Range II
0.0020	3.0	0.5 for TMDSC 0.0 for DSC	60.0	0.040	10.0	1.50 0.055	3.0 0.070	1.50 0.055

When there are endo- and exo-thermal events such as melting, crystallization, curing, and chemical reaction for the sample during an experiment, Eq. (1) might not necessarily be analytically solvable. In such a case, numerical solutions can be obtained by employing a Runge-Kutta method.[12,13,17–19]

RESULTS AND DISCUSSION

The above equations allow one to model DSC and TMDSC output curves for samples with known (assumed) thermal properties and known (assumed) instrumental/experimental parameters such as λ, ω, and C_{pr}. This technique is free from experimental errors and there is no need for instrumental calibration; in addition, we know the sample properties exactly.

Table I displays the thermal properties of a sample as well as all the other conditions under which a DSC and TMDSC experiment can be carried out. The experimental conditions are chosen within the range of actual experiments in materials characterization practice, but the sample has been assumed to have two-step changes in its specific heat over the temperature ranges, as shown in Figure 1. The DSC and TMDSC curves showing the output heat flow were obtained as the analytical solution of eq. (2) and are displayed in Figure 2. An upward shifting corresponding to the initial transient period can be observed for the curves. This transient period is usually cut off by starting an experiment, using an actual DSC or TMDSC, at lower temperature in common practice. The second and third transient periods starting at the beginning of temperature Ranges I and II, however, are not avoidable. Therefore, there are certain degrees of distortion between the measured curves and the thermal property of the sample in DSC measurement. This is caused by the intrinsic nature of thermal transfer, which is determined by the Newton's cooling law. The greater the thermal transfer coefficient, the smaller the transient effect. The equilibrium part of the underlying heat flow doubles in Range I as the heat capacity difference between the sample and reference is doubled, regardless of the heat capacity of reference, C_{pr}, and the thermal transfer coefficient, λ.

The TMDSC output curve consists of a sinusoidal-like continuous curve superimposed on the DSC curve. Note that the upper and lower envelops represent neither the heat flows obtained using a conventional DSC at the heating rates $q + A_b$ and $q - A_b$; nor that at $(q + A_b)/\omega$ and $(q - A_b)/\omega$. The amplitude of heat flow is seen to increase with increasing the heat capacity of the sample, but not in a linear manner, i.e., doubling the heat capacity of the sample (excluding

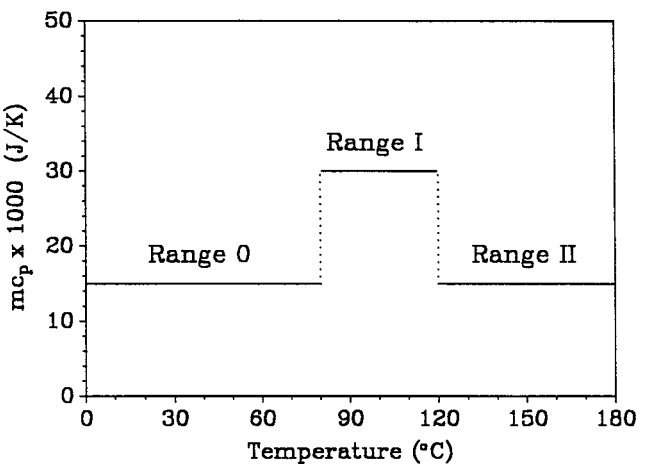

Figure 1 An assumed sample whose specific heat has two-step changes over the temperature ranges.

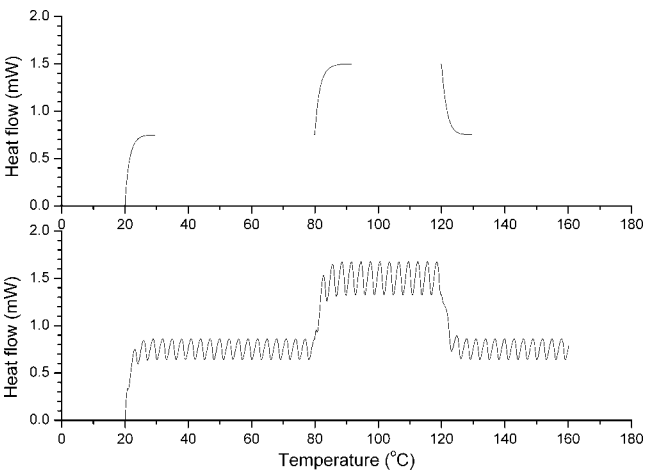

Figure 2 Computed DSC and TMDSC output curves for the sample shown in Figure 1 under experimental conditions listed in Table I.

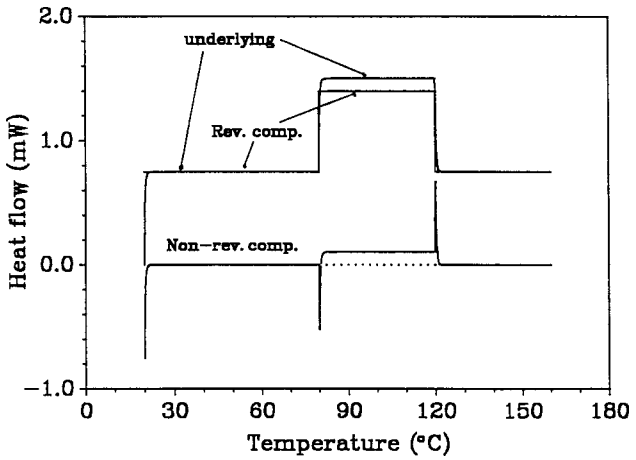

Figure 3 Underlying heat flow and separated reversing and nonreversing heat flows for the TMDSC curve shown in Figure 2.

the heat capacity of pan) does not result in doubling of the amplitude (0.354263 mW vs. 0.221748 mW).

The TMDSC output curve was further analyzed to obtain reversing and nonreversing components using the method discussed in the literature (e.g., Refs. 3, 14), which are shown in Figure 3. One observes clearly a nonreversing curve—this is contradictory with the experimental assumptions. Table I specifies that the heat capacity of the sample depends on temperature only irrelevant with any other factors. Thus, the nonreversing component is purely a by-product originating from the specific way of the measurement rather than from the sample. One may try to apply a calibration to avoid this discrepancy. However, one will find there is no constant simultaneously suiting both for Ranges 0 and II and for Range I. The two spikes at 80 and 120°C are due to the transient effect caused by two discontinuous changes in specific heat of the sample. This example highlights why deconvolution of the reversing and nonreversing components is artificial.

Schawe pointed out that there might be problems in the interpretation of the reversing and nonreversing components.[5] He argued that the fundamental equation adopted in such analysis is valid only for time-independent thermal events. In addition, he developed an alternative method based on the linear-response theory to analyze the oscillating heat flow.[20–24] The phase lag between the oscillating heat flow and the modulated scanning temperature program [Eq. (4)] is measured; and the ''storage heat capacity'' and ''loss heat capacity'' are then calculated, in analog of the storage modulus and loss modulus that are used in DMA. The modulus of the complex heat capacity, the storage, and loss heat capacities have been calculated,[20–24] and displayed in Table II. Clearly, C_{ps}, calculated from the conventional DSC curves (the third row in Table II) returns figures (0.015, 0.030, and 0.015) exactly the same as the assumed figures (the second row in Table II or Table I). The modulus of Schawe's complex heat capacity, $|C^*|$, however, is not equal to the heat capacity of the sample (excluding pan). This suggests that the storage and loss heat capacities are not physically meaningful.

We can further simulate DSC and TMDSC curves for polymer melting. Assume a sample with its melting temperature at 100°C and its crystallites having such a size distribution that the melting temperature spans from 80 to 120°C with a Gaussian prifile.[13] Table III summarizes the sample properties and DSC and TMDSC experimental conditions. The specific heat of the sample is a constant over the whole temperature range apart from the melting.

Where, the new symbols are defined as follows:

ΔH_m^0 (J/g) – Melting enthalphy
χ (%) – Crystallinity:
T_{max} (°C) – Peak melting temperature
μ_m^2 – Half width of distribution:

The output curves for the DSC and TMDSC experiments were computed [eq. (2)] using a Runge-Kutta method[13] and are shown in Figures 4 and 5, respectively. An endotherm corresponding to the melting of crystallites is observed, a rather familiar experimental result to thermal analysts. For the

TABLE II
Computed Complex Heat Capacity Using a Method in the Literature

	$C_{ps} - C_{pr} = mc_{ps}$ at Range 0	$C_{ps} - C_{pr} = mc_{ps}$ at Range I	$C_{ps} - C_{pr} = mc_{ps}$ at Range II
Assumed value (J/K)	0.0150	0.0300	0.0150
Computed from the DSC curve (J/K)	0.0150	0.0300	0.0150
Modulus of complex heat capacity $\|C^*\|$	0.01199	0.02232	0.01199
Phase lag δ (degree)	−37.33	−31.03	−37.33
Storage heat capacity C'	−0.00727	−0.01150	−0.00727
Loss heat capacity C''	0.00953	0.01912	0.00953

TABLE III
Numerical Simulation Conditions and Thermal Properties of the Sample

λ (J/K s)	q (°C/min)	A_b (°C)	p (s)	C_{pr} (J/K)	m (mg)	c_{ps} (J/g K) in Ranges 0, I, and II	ΔH_m^0 (J/g)	χ (%)	T_{max} (°C)	μ_m^2
0.0020	5.0	0.50 for TMDSC 0.0 for DSC	30.0	0.040	10.0	1.50	30.0	84.15	100.0	250.0

TMDSC curve, the sinusoidal fluctuation of heat flow that results from modulation of heating rate is seen up and down around the underlying heat flow. Subtracting the underlying heat flow from the TMDSC heat flow leads to the amplitude plot that is shown in Figure 6. The amplitude expands, reaches the maximum, and then recovers as the melting of crystallites ends.

The curve is deconvoluted to obtain the reversing and nonreversing components following the method discussed in the literature.[3,11] Both the reversing and nonreversing components are obtained and shown in Figure 7. This nonreversing component is contradictory with the original assumption, indicating that the separation of the reversing and nonreversing components is not physically meaningful.

Common misconceptions

Many thermal analysts have experienced difficulties in consistently interpreting their TMDSC results. Nevertheless, the reason for the difficulties has not been well understood. To have an improved knowledge of TMDSC, it is necessary to clarify some commonly shared misconceptions, which have dominated the way of our thinking.

DMA and TMDSC

A reason why one easily believes TMDSC has intrinsic advantages over a conventional DSC comes from the comparison of TMDSC with DMA (dynamic mechanical analysis), in which a sinusoidal stress (or strain) is applied to a sample, and response strain (or stress) is measured as a function of time. The advantages of DMA over TMA (thermal mechanical analysis), in which a constant stress/strain is applied to a sample, are well known. Modulation of loading force (or strain) has allowed one to measure the dynamic performance of a sample.

The phase lag in DMA has a different origin from that of TMDSC. Modulated external force (or strain) transmits instantaneously (or at the sound velocity of the sample) to the whole sample, and the phase lag of response strain (or stress) is caused by the viscous property of the sample. Two independent physical parameters, elasticity, G, and viscosity, η, are required to characterize a viscoelastic sample. Modulation of loading force enables the viscoelastic property to be measured. According to either the Maxwell model, or the Voigt model or other more sophisticated models, one extracts information on the sample from the storage modulus, G', and the loss modulus, G''; or from the modulus of the complex modulus, $|G^*|$, and the

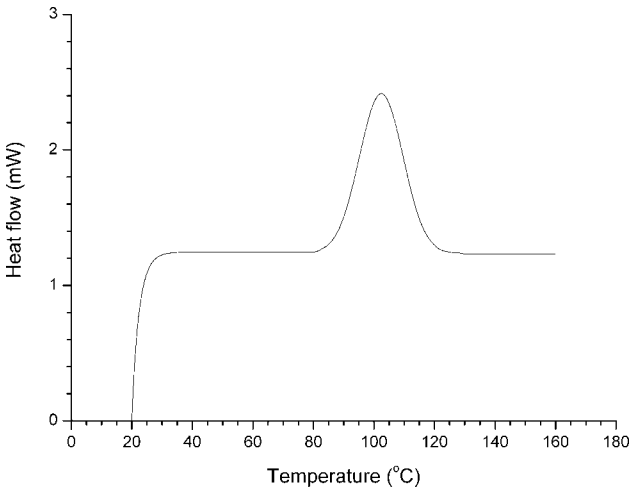

Figure 4 Computed DSC output curve for melting of a sample with Gaussian distribution in crystallite size that results in corresponding distribution in melting temperature.

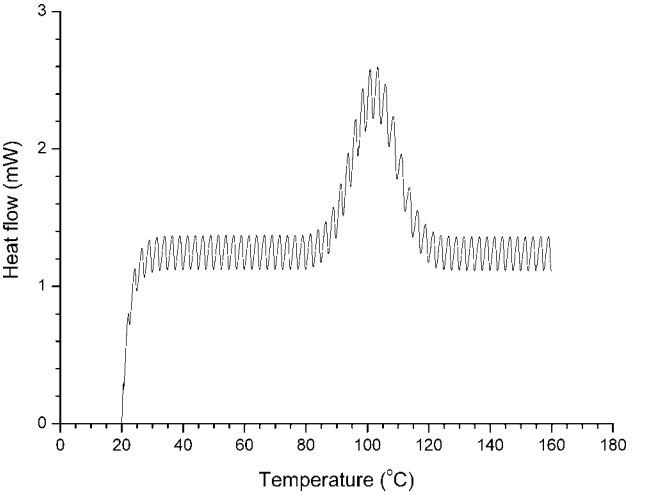

Figure 5 Computed TMDSC output curve for melting of the same sample used for Figure 4 under conditions shown in Table III.

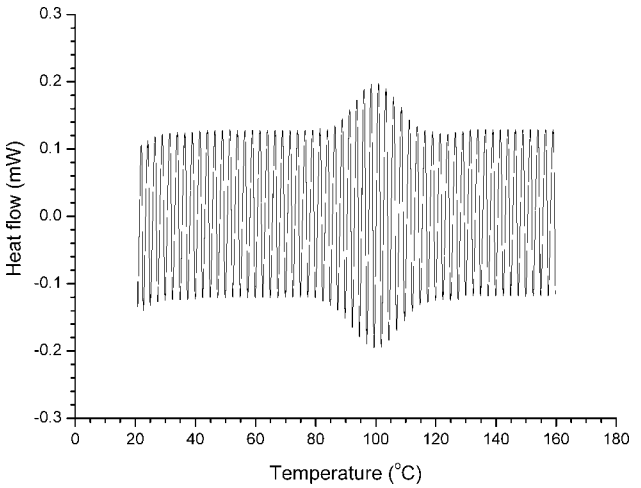

Figure 6 Amplitude plot obtained by subtracting the underlying heat flow from the heat flow of TMDSC curve shown in Figure 5.

phase lag between the applied loading and the measured response, δ. The expressions for the most popular Maxwell model read,

$$G^* \equiv G' + iG'' \tag{5}$$

$$|G^*| \equiv \sqrt{G'^2 + G''^2} = G\frac{\omega\tau}{\sqrt{1+\omega^2\tau^2}} \tag{6}$$

$$\tau \equiv \frac{\eta}{G} \tag{7}$$

$$G' = G\frac{\omega^2\tau^2}{1+\omega^2\tau^2} \tag{8}$$

$$G'' = G\frac{\omega\tau}{1+\omega^2\tau^2} \tag{9}$$

$$\tan\delta \equiv \frac{G''}{G'} = \frac{1}{\omega\tau} \tag{10}$$

where τ is the relaxation time constant and ω denotes the angular frequency of applied sinusoidal loading.

It is important to note that the complex modulus, storage modulus, and loss modulus are no longer the ''modulus'' with original physical definition, i.e., Young's modulus. There are only three independent parameters in eqs. (5–10); two of them (G, η) reflect the characteristics of a sample, and the other (ω) is an experimental parameter. The other parameters can always be expressed as a function of these three independent variables.

On the other hand, the phase lag observed from a TMDSC measurement originates from the time difference for thermal transfer from the heating block to sample and reference, which is a characteristic of measurement. A quantitative description of the phase lag is shown in eq. (4). There is only one independent parameter ($=C_{ps} - C_{pr}$) characterizing the sample, the others originate from the measurement itself. In a conventional DSC, the ''instrumental factors,'' λ and C_{pr} are cleverly removed from the output heat flow by ''differential,'' permitting extraction of information on the sample measured, provided the transient term has decayed to an acceptable level [see eq. (2)]. The departure of heating rate from constant in the case of TMDSC has unnecessarily complicated the quantitative relationship between the output results and input conditions. Thus, the in-phase and out-phase components, or ''real heat capacity'' and ''imaginary heat capacity'' or ''storage heat capacity'' and ''loss heat capacity'' do not provide a basis for characterizing the measured thermal properties of samples.

Further discussion on heat capacity

In spite of the fact that the heat capacity is a well-defined physical concept, the apparent similarity of TMDSC and DMA has led to the definition of complex heat capacity in analog of DMA [e.g., Refs. 5, 20–24],

$$C^*(\omega) \equiv C'(\omega) - iC''(\omega) \equiv |C^*|e^{-i\delta(\omega)} \tag{11}$$

where δ is the phase shift between the oscillating component of the output heat flow and the applied modulation of heating program.

The quantities defined as the modulus of the complex heat capacity, storage heat capacity (real part), and loss heat capacity (imaginary part) are not the ''heat capacity'' with the original physical definition. These terminologies can only be used for describing mathematical manipulations using the complex number. In many cases, however, these words have been used as a physical essence to discuss the material characteristics of a sample. It has been claimed that the real

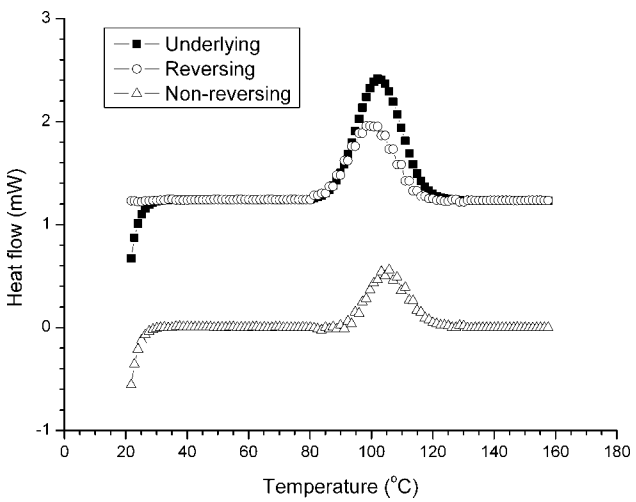

Figure 7 Underlying heat flow and separated reversing and nonreversing components for the TMDSC experiment shown in Figure 5.

part of the complex heat capacity, C', describes molecular motions and corresponds to the heat capacity in the case of equilibrium C_p; the imaginary part, C'', is linked to dissipation processes or surface melting.[5,20–24] The word ''frequency dependent heat capacity'' has appeared in various publications.[25–29]

Gmelin[29] further stated ''the essential implication of TMDSC originates from the fact that, besides the temperature-dependent heat capacity, the frequency-dependence of heat capacity becomes involved.'' The symbol $C(T, \omega)$ has been employed to describe this idea. In fact, the storage and loss heat capacity has been employed to discuss the materials characteristics in polymer melting, crystallization, etc.[9,20–24] Note that this frequency is not the frequency of crystal lattice vibration occurring in a sample, as discussed in the Einstein model and the Debye model.[30] It is the modulation frequency of heating program, which practically varies in a narrow range of approximate 10–100 s in terms of the modulation period.

These statements are misleading. Besides, the reasons already explained in Section DMA and TMDSC, one may ask what occurs if we heat up a sample with unit mass from temperature T_1 to T_2 with frequency ω_1, then cool the sample down from T_2 to T_1 with frequency ω_2. An accurate mathematical expression reads

$$\Delta H = \int_{T_1}^{T_2} C(T, \omega_1) dT + \int_{T_2}^{T_1} C(T, \omega_2) dT = \int_{T_1}^{T_2} [C(T, \omega_1) - C(T, \omega_2)] dT \neq 0 \; ? \qquad (12)$$

Presumably, no one intends to claim another ''permanently working machine'' as somehow implied by the term ''frequency dependent heat capacity.''

There are a number of publications reporting frequency dependency of the glass transition, and the frequency dependency of the heat capacity at the glass transition region. For instance, Montserrat found that the glass transition temperature determined according to the modulus of the complex heat capacity, $|C_p^*|$ (called dynamic glass transition by Montserrat), is frequency dependent while that determined according to the total heat flow (conventional DSC) is not.[31] This article, however, will not make further comments on these in either way. It requires elaborate analysis and discussion case by case.

CONCLUSION

Although modulation has been proven to be a useful technique in various fields including AC calorimetry, the physical meaning of temperature modulation for DSC is another matter. DSC and TMDSC output curves are computable either analytically or numerically, and the TMDSC output heat flow can be further separated to obtain the reversing and nonreversing heat flows. It has been found that separation of the reversing and nonreversing heat flows is artificial. No additional physical parameter of a test sample is measured in TMDSC; instead departure of the heating rate from constant results in abdication of the smartest innovation of DSC, ''differential.'' It is also concluded that neither the use of the ''storage heat capacity,'' C', nor ''loss heat capacity,'' C'', is physically meaningful.

References

1. Reading, M.; Elliot, D.; Hill, V. L. J Therm Anal, 1993, 40, 949.
2. Reading, M. Trends Polym Sci 1993, 8, 248.
3. Wunderlich, B.; Jin, Y.; Boller, A. Thermochim Acta 1994, 238, 277.
4. Hatta, I. Jpn J Appl Phys 1994, 33, L686.
5. Schawe, J. E. K. Thermochim Acta 1995, 260, 1.
6. Cao, J.; Yu, L.; Shanks, R. A. J Therm Anal 1997, 50, 365.
7. Ozawa, T. Thermochim Acta 1995, 253, 183.
8. Ozawa, T.; Kanari, K. Thermochim Acta 1996, 288, 39.
9. Saruyama, Y. In Proceedings of the 11th International Congress on Thermal Analysis and Calorimetry, Philadelphia, August 12–16, 1996; p 139.
10. Lacey, A. A.; Nikolopoulos, C.; Reading, M. J Therm Anal 1997, 50, 279.
11. Boller, A.; Jin, Y.; Wunderlich, B. J Therm Anal 1994, 42, 307.
12. Cao, J. Thermochim Acta 1999, 325, 101.
13. Cao, J. Thermochim Acta 1999, 329, 89.
14. Xu, S. X.; Li, Y.; Feng, Y. P. Thermochim Acta 2000, 343, 81.
15. Cao, J. Presented at the 5th Lhnwitz Seminar on Calorimetry, Rostock, Germany, June 7–12, 1998.
16. Clarke, S.; Folland, P.; Matisons, J.; Thermochim Acta 2000, 351, 29.
17. Cao, J. Polymer 1992, 33, 3520.
18. Cao, J.; Buckley, A. N.; Lynch, L. J. Carbon 1994, 32, 493.
19. Cao, J.; Kikutani, T.; Takaku, A.; Shimizu, J. J Appl Polym Sci 1989, 37, 2683.
20. Schawe, J. E. K. Thermochim Acta 1995, 260, 183.
21. Schawe, J. E. K. Thermochim Acta 1996, 271, 127.
22. Schawe, J. E. K.; Bergmann, E. Thermochim Acta 1997, 304/305, 179.
23. Schawe, J. E. K.; Hohne, G. W. H. J Thermal Anal 1996, 46, 893.
24. Merzlyakov, M.; Schick, C. Thermochim Acta 1999, 330, 55.
25. Kamasa, P.; Merzlyakov, M.; Pyda, M.; Pak, J.; Schick, C.; Wunderlich, B. Thermochim Acta 2002, 392/393, 195.
26. Kamasa, P.; Pyda, M.; Buzin, A.; Wunderlich, B. Thermochim Acta 2003, 396, 109.
27. Schick, C.; Wurm, A.; Mohamed, A. Thermochim Acta 2002, 392/393, 303.
28. Carpentier, L.; Bustin, O.; Descamps, M. J Phys D: Appl Phys 2002, 35, 402.
29. Gmelin, E. Thermochim Acta 1997, 304/305, 1.
30. Wunderlich, B. Thermochim Acta 1997, 300, 43.
31. Montserrat, S. J Therm Anal Calorim 2000, 59, 289.